GDCh

Research Articles

Angewandte
Chemie
International Edition
www.angewandte.org

Main Group Chemistry | Hot Paper

Isolation of an Annulated 1,4-Distibabenzene Diradicaloid

Henric Steffenfauseweh, Dennis Rottschäfer, Yury V. Vishnevskiy, Beate Neumann,
Hans-Georg Stammler, Dariusz W. Szczepanik, and Rajendra S. Ghadwal*

Dedicated to Professor Douglas W. Stephan on the occasion of his 70th birthday

Abstract: The first 1,4-distibabenzene-1,4-diide compound $[(ADC)Sb]_2$ (**5**) based on an anionic dicarbene (ADC) (ADC = PhC{N(Dipp)C}$_2$, Dipp = 2,6-iPr$_2$C$_6$H$_3$) is reported as a bordeaux-red solid. Compound **5**, featuring a central six-membered C$_4$Sb$_2$ ring with formally Sb^I atoms may be regarded as a base-stabilized cyclic bis-stibinidene in which each of the Sb atoms bears two lone-pairs of electrons. **5** undergoes 2e-oxidation with Ph$_3$C[B(C$_6$F$_5$)$_4$] to afford $[(ADC)Sb]_2[B(C_6F_5)_4]_2$ (**6**) as a brick-red solid. Each of the Sb atoms of **6** has an unpaired electron and a lone-pair. The broken-symmetry open-shell singlet diradical solution for (**6**)$^{2+}$ is calculated to be 2.13 kcal mol^{-1} more stable than the closed-shell singlet. The diradical character of (**6**)$^{2+}$ according to SS-CASSCF (state-specific complete active space self-consistent field) and UHF (unrestricted Hartree-Fock) methods amounts to 36% and 39%, respectively. Treatments of **6** with (PhE)$_2$ yield $[(ADC)Sb(EPh)]_2[B(C_6F_5)_4]_2$ (**7**-E) (E = S or Se). Reaction of **5** with (cod)Mo(CO)$_4$ affords $[(ADC)Sb]_2Mo(CO)_4$ (**8**).

Introduction

Benzene is the most intensively studied 6π-electron aromatic hydrocarbon.[1] It has also been an intriguing structural motif in fundamental main-group chemistry.[2] Like benzene, pyridine (C$_5$H$_5$N) follows the Hückel criteria for aromatic systems and is thermally stable.[1] However, the thermal stability of heavy heteroarenes C$_5$H$_5$E and related unsaturated species decreases accordingly to E = P > As > Sb > Bi.[3] This trend is usually attributed to weak C=E π-interaction, making these species highly reactive and hence prone to oligomerize or decompose.[4] Consequently, isolable bismaalkene[5] and stibaalkene[6] species are rather scarce

compared to arsaalkene[7] and phosphaalkene compounds.[8] Since the isolation of the first phosphabenzene, 2,4,6-Ph$_3$C$_5$H$_2$P, by Märkl in 1966,[9] several stable compounds featuring one or more two-coordinated phosphorus or arsenic atom(s) in a six-membered unsaturated ring have been reported.[8b,10] Over the past years, phosphabenzene derivatives have attracted interests as ligands in organometallic chemistry and catalysis.[10g,11] In contrast, stable stibabenzene and bismabenzene species remained extremely rare.[12] In this context, the pioneering work by Ashe III is striking.[3a–d] In 1971, Ashe III et al. reported on the synthesis and low temperature spectroscopic details of the parent stibabenzene **I**-H (Figure 1), which was found to be extremely labile and readily polymerized to an intractable

[*] H. Steffenfauseweh, Dr. D. Rottschäfer, Dr. Y. V. Vishnevskiy,
B. Neumann, Dr. H.-G. Stammler, Priv.-Doz. Dr. R. S. Ghadwal
Molecular Inorganic Chemistry and Catalysis, Inorganic and
Structural Chemistry, Center for Molecular Materials, Faculty of
Chemistry, Universität Bielefeld
Universitätsstrasse 25, 33615 Bielefeld (Germany)
E-mail: rghadwal@uni-bielefeld.de
Homepage: www.ghadwalgroup.de

Dr. D. W. Szczepanik
Department of Theoretical Chemistry, Faculty of Chemistry, Jagiellonian University
Gronostajowa 2, 30-387 Kraków (Poland)

Dr. D. Rottschäfer
Current address: Department of Chemistry, Philipps-University
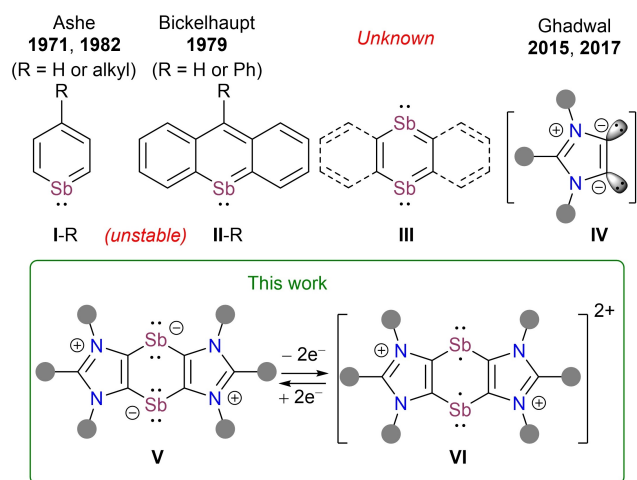Marburg
Hans-Meerwein-Str. 4, Marburg (Germany)

*Figure 1.* Selected early examples of antimony heterocycles **I**-R and **II**-R.

brown tar at temperatures above −80 °C.[13] Later, the same research group also prepared 4-alkyl substituted stibabenzene derivatives **I**-R.[14] While **I**-R were proposed to exist in equilibrium with their Diels–Alder dimers below −70 °C, they immediately decomposed at higher temperatures. A similar observation was made by Bickelhaupt while attempting to prepare stibaanthracene (**II**).[15] In 2016, Yamashita et al. isolated the first crystalline bismabenzene, i.e., 2,5-(iPr₃Si)₂C₅H₃Bi.[12] To the best of our knowledge, a related stable antimony compound has not been reported to date.

Pyrazine (1,4-diazabenzene) and related benzo-annulated N-heterocycles have attracted considerable attentions as key structural motifs for N-doped polycyclic aromatic hydrocarbons (PAHs) relevant to materials applications.[16] Phosphorus and arsenic analogues of pyrazine are scarce,[8b,10] while related mono-, bi, or tricyclic antimony species such as **III** remained virtually unknown. This emphasizes the need of new precursors and synthetic methodologies to access this class of compounds. Very recently, we introduced a fundamentally new type of carbon-donor frameworks, namely vicinal anionic dicarbenes (ADCs, **IV**), for accessing stable main-group heterocycles. The ADCs (**IV**) are prepared in near quantitative yields by the double deprotonation of C2-arylated 1,3-imidazolium salts.[17] The structure of **IV** in the solid-state is

yet to determine, we have already shown the suitability of **IV** in the synthesis of phosphorus,[10h,18] arsenic,[19] germanium,[20] and tin[21] containing heterocycles. Herein, we report the synthesis and structural characterization of the first 1,4-distibabenzene-1,4-diide compound **V** and its two electron (2e)-oxidation product **VI**, the ionic 1,4-distibabenzene species by the use of an ADC (**IV**).

Results and Discussion

The desired starting compound [(ADC)SbCl₂]₂ (**4**) (ADC = CPh{N(Dipp)C}₂, Dipp = 2,6-iPr₂C₆H₃) is prepared as a colorless crystalline solid by reacting C4,C5-bis-silylated-1,3-imidazolium chloride (**3**)[10h] with SbCl₃ (Scheme 1).[22] Treatment of **4** with 4 equivalents of KC₈ affords **5** as a bordeaux-red crystalline solid in 90 % yield. Like (L)SbCl₂R (L = N-heterocyclic carbene (NHC) or cyclic alkyl amino carbene (cAAC), R = Cl, aryl or OTf),[23] **4** may be regarded as a Lewis acid-base adduct with four-coordinated antimony(III) atoms.[24] Note, the ADC serves as a monoanionic four-electron donor (LX-type) ligand. Each of the antimony atoms of **5** is in a formal oxidation state of +1 and has two lone-pairs of electrons. Thus, like Lewis base-stabilized neutral (**VII–XII**)[23c,d,25] and cationic (**XIII**)[26] stibinidene
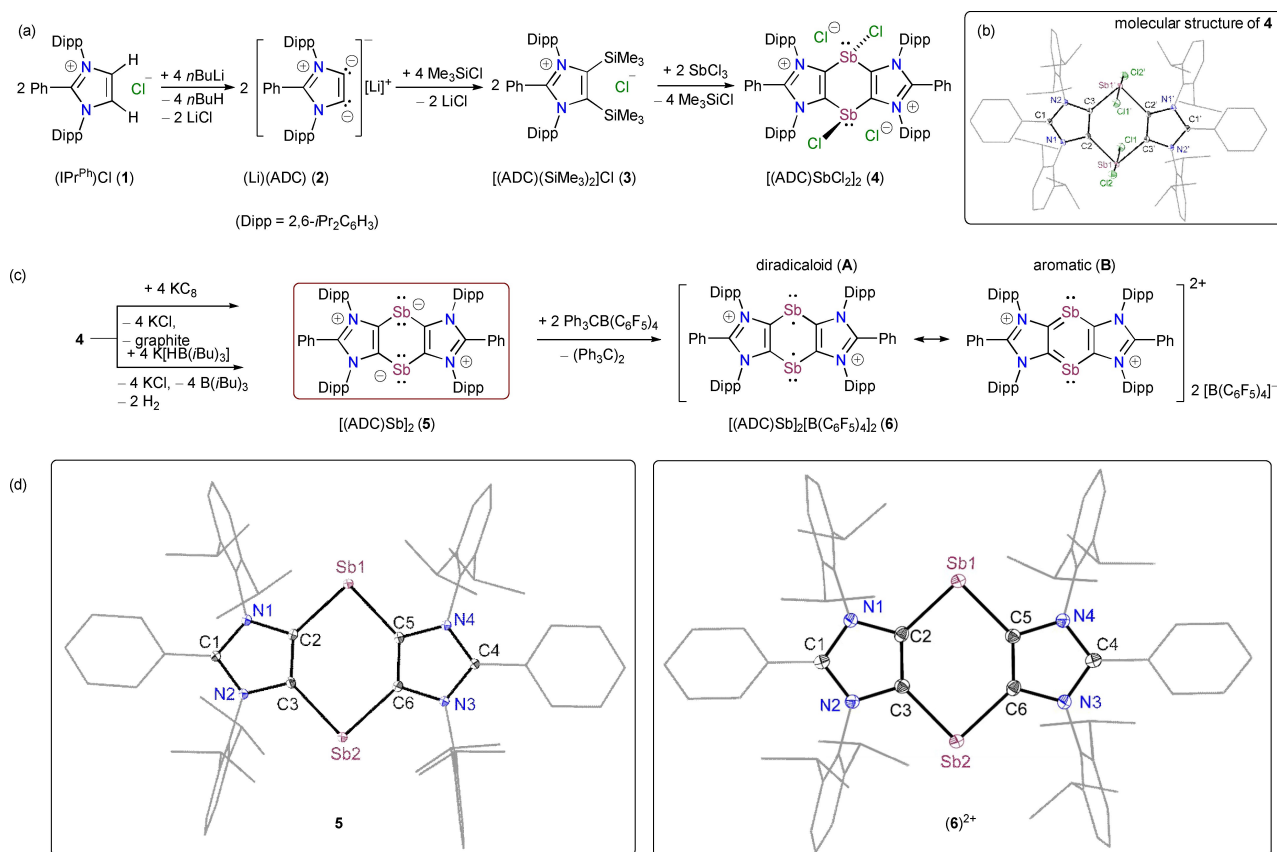
Scheme 1. a) Synthesis of **4**. b) Solid-state molecular structure of **4** (at 100 K). Thermal ellipsoids are displayed at the 50 % probability level. H atoms are omitted. Aryl substituents are depicted as wire-frame models for clarity. c) Synthesis of **5** and **6**. d) Solid-state molecular structures of **5** and (**6**)²⁺ (at 100 K). Aryl substituents are shown as wire-frames. Solvent molecules and H atoms (and B(C₆F₅)₄ anions for **6**) have been omitted for clarity.

compounds (Figure 2), **5** may be regarded as a rare example of base-stabilized cyclic bis-stibinidene species. The weight of major resonance structures (see a–c for **IX**, Figure 2) depends on the π-acceptor property of the singlet carbene. In 2010, Dostál et al. prepared a crystalline stibinidene compound **XI** derived from a monoanionic NCN-pincer ligand (L_{NCN}).[27] Later, they showed the use of **XI** as a 2e-donor ligand for transition metals.[28] **XI** was prepared by reacting (L_{NCN})SbCl₂ with potassium selectride K[HB(iBu)₃] to generate the hydride (L_{NCN})SbH₂, which immediately decomposed into **XI** and dihydrogen.[27] Similarly, treatment of **4** with four equivalents of K[HB(iBu)₃] also affords compound **5** in an almost quantitative yield.

Like related phosphorus[10h] and arsenic[19] compounds, one of the lone-pairs of each antimony atom in a p-type orbital of **5** may be partially delocalized into the C_4Sb_2 ring, giving rise to a formal 8π-electron antiaromatic system (see below). Compound **5** readily undergoes 2e-oxidation with Ph₃C[B(C_6F_5)₄] to form the dicationic compound **6** as a brick-red crystalline solid in 81 % yield.[29] **6** features two di-coordinated antimony atoms, each bearing an unpaired electron (see the diradicaloid form **A**) and a lone-pair. The two unpaired electrons may delocalize into the C_4Sb_2 ring to form a 6π-electron benzenoid (aromatic) species (**B**) (see below for further details).

The ¹H and ¹³C NMR spectra of **4**, **5**, and **6** exhibit expected signals for the ADC moiety. The NMR signals of compounds **4**–**6** are fully consistent with their solid-state molecular structures (Scheme 1)[30] established by single-crystal X-ray diffraction and suggest highly symmetric environments around the C_4Sb_2 core. Notably, the ¹³C NMR signal for the *C*Sb moiety in **6** (164.9 ppm) is downfield shifted with respect to that of **5** (149.3 ppm), suggesting an aromatic ring current effect in the former.[10h,19–21]

The solid-state molecular structure of **4** features a six-membered C_4Sb_2 ring in which each of the four-coordinated antimony atoms adopts a seesaw molecular geometry as observed for Sb^III Lewis adducts (L)SbCl₂R (L = NHC or cAAC, R = Cl, aryl or OTf).[23] Note, the ADC in **4** is a monoanionic four-electron donor. Both the chlorine atoms occupy axial positions. The Sb1–Cl1 (2.680(1) Å) and Sb1–Cl2 (2.500(1) Å) bond lengths of **4** compare well with

the axial Sb–Cl$_{ax.}$ bond lengths of (L)SbCl₂R (2.50 to 2.64 Å).[23] These values are slightly longer than the Sb–Cl covalence (2.39 Å)[31] but shorter than the sum of the van der Waals (vdW) radii (4.00 Å).[32] The Wiberg bond indices (WBIs) for Sb–Cl bonds of **4** amount to 0.42 and 0.52 (see also Tables S9 and S10 for natural bond orbital (NBO) analyses). Thus, the Sb–Cl bonds of **4** may primarily be considered of ionic nature. The Sb–C bond lengths of **4** (2.154(1)–2.156(1) Å) (Table 1) are slightly shorter than those of the related acyclic Sb^III compounds (L)SbCl₂R (2.193(6) to 2.367(6) Å, L = NHC or cAAC).[24] This may be attributed to the stronger σ-donor property of ADCs than NHCs and cAACs.[33] The Sb–C bond lengths of **4** are in the range of the Sb–C$_{aryl}$ bond lengths (2.159(3)–2.18(3) Å) measured for (L)SbCl₂R (R = aryl).[24] The C–Sb–C bond angle of **4** (94.8(1)° is smaller than the C–Sb–C$_{aryl}$/Cl$_{eq.}$ (96.70(5) to 104.5(2)°) angles of (L)SbCl₂R.[24] This may be ascribed to the cyclic structure of **4**.

The C–Sb bond lengths of **5** (2.139(2)–2.142(2) Å) are akin to that of the base-stabilized cationic stibinidene [(cAAC)₂Sb]⁺ (**XIII**) (2.145(2) Å).[26] It should be noted that cAACs are better electrophiles than NHCs, while ADCs and C4-carbenes are poorer π-acceptors than NHCs.[33] Thus, a modest Sb–C double bond character in **5** may be anticipated (see below the NBO analyses). The Sb–C bonds of **6** (2.088(2)–2.094(2) Å) are shorter than those of **4** and **5**. This may be attributed to the delocalization of the antimony unpaired electrons over the C_4Sb_2 ring, thus resulting in a higher C–Sb bond order in **6**. This feature is consistent with the delocalization of the unpaired (or lone-pair) electron of dicationic (or neutral) phosphorus[10h] and arsenic[19] as well as neutral germanium[20] and tin[21a] compounds containing a planar C_4E_2 ring (E = P, As, Ge, Sn).

The C–Sb bond length of **6** (2.088(2)−2.094(2) Å) matches well with Bertrand's base-stabilized stibinidene-(cAAC)SbCl (2.082(5) Å)[23c] featuring a good π-acceptor cAAC as well as the calculated value for the parent stibabenzene **I-H** (2.05 Å).[34] Moreover, this value of **6** is also close to the C=Sb bond length calculated for HSb=CH₂ (1.99 Å)[35] as well as of the rare 2,3-distibabutadienes [R(Me₃SiO)C=Sb]₂ (R = 2,4,6-Me₃C₆H₂, 2.056(10) Å or 2,4,6-tBu₃C₆H₂, 2.065(5) Å).[3h] In line with the Sb–C bond length descending trend, the C–C bond lengths increase from **4** to **5/6** (Table 1), which suggests increasing π-
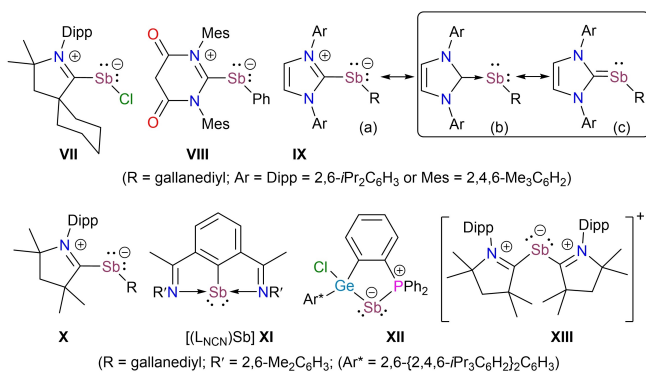
Figure 2. Structurally characterized Lewis base-stabilized neutral **VII–XI** (with major resonance forms a-c for **IX**) and cationic **XI** stibinidenes.

Table 1: Selected bond lengths [Å] and bond angles [°] of compounds **4**, **5**, and **6**.

	4	5	6
Sb–C	2.154(1)–2.156(1)	2.139(2)–2.142(2)	2.088(2)–2.094(2)
C–C	1.361(2)	1.385(2)–1.386(2)	1.390(3)
N–C	1.399(2)–1.403(2)	1.396(2)–1.400(2)	1.404(3)–1.413(3)
N–C′	1.350(2)–1.355(2)	1.364(2)–1.367(2)	1.344(3)–1.354(3)
C–Sb–C	94.8(1)	90.8(1)	91.5(1)
C–C–Sb	130.4(1)	134.2(2)	132.3(2)
Angles[a]	9.3(1)/0	5.4(1)/11.5(1)	0/0

[a] Plane angles between 1,3-imidazole and C_4Sb_2/1,3-imidazole ring-planes.

conjugation from **4** to **6**. The C_4Sb_2 ring in **4–6** is almost planar. The angle between the planes of 1,3-imidazole and C_4Sb_2 rings decreases from **4** to **6**. So, both 1,3-imidazoles as well as to some extent the C_4Sb_2 ring of **6** become flattened. The C–Sb–C angle of **6** (91.5°) matches with the calculated value for **I**-H (93°)[34] The Sb···Sb distance in **6** (4.304(1) Å) is larger than the sum of the antimony covalent radii (2.812 Å)[31] but smaller than the sum of the vdW radii (4.50 Å).[32] This feature correlates well with other main-group diradicaloids.[36]
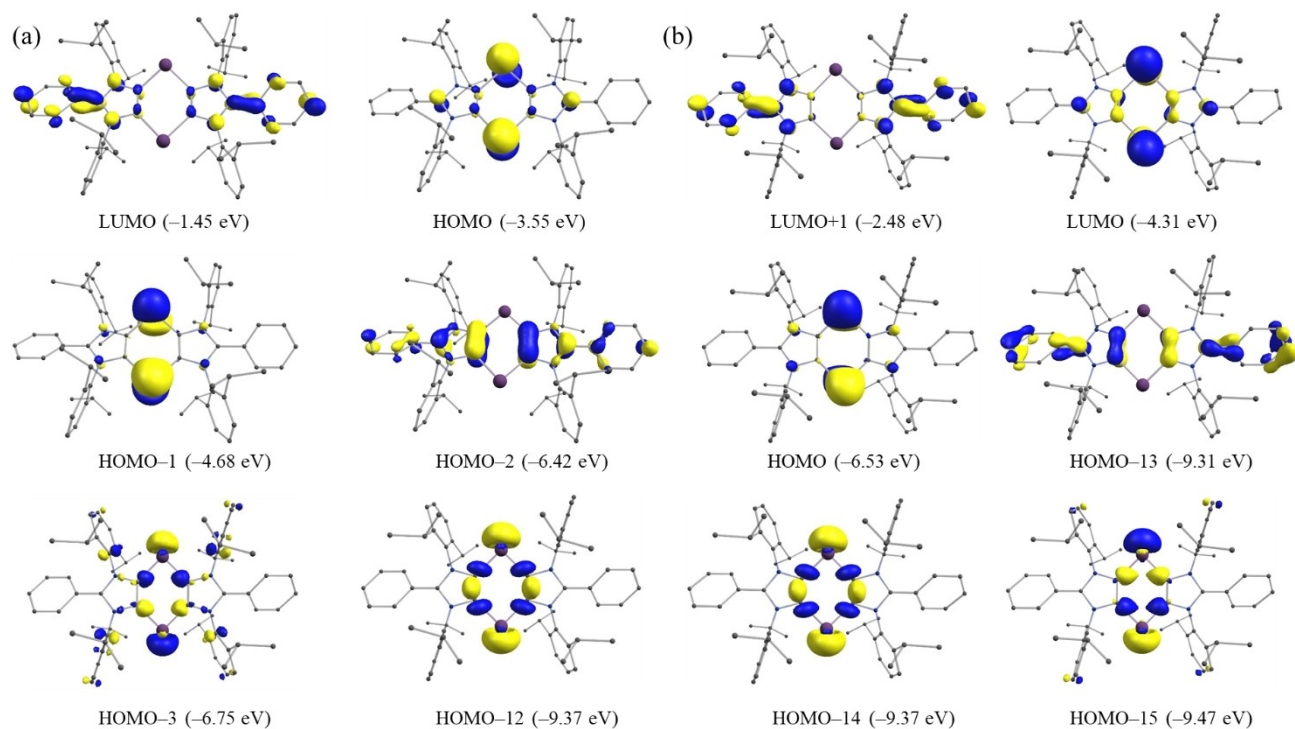
To obtain further insights into the electronic structures of **5** and **6**, we performed quantum chemical calculations. The DFT optimized structures of **5** (Figure S38) and $(6)^{2+}$ (Figure S39) at the PBEh-3c level are in good agreement with the XRD structures (Scheme 1d). According to NBO analyses, the natural atomic charges (Table 2) on antimony atoms of **4** (1.28), **5** (0.30), and $(6)^{2+}$ (0.97) are consistent with their formal oxidation states. The WBIs for the C–Sb bond of **5** (0.89) and $(6)^{2+}$ (0.99) suggest increasing bond order and hence larger π-delocalization in the latter. This is in line with the Sb–C bond lengths of **5** and $(6)^{2+}$ (Table 1).

The HOMO and HOMO–1 of **5** are the π-type lone-pair orbitals, while the HOMO–3 and HOMO–12 are the remaining two low-lying σ-type lone-pair orbitals at the antimony atoms (Figure 3a). The LUMO of **5** is essentially on the 1,3-imidazole ring and C2-phenyl substituent. The HOMO–2 of **5** is mainly located at the C=C bonds of 1,3-imidazole rings with some contribution from the C2-phenyl substituents. A similar orbital topology was also seen for the related arsenic derivative with a C_4As_2 ring.[19] Akin to the base-stabilized stibinidenes, Mujumdar et al. reported a cyclic two-coordinated Sb^I cation, derived from 5,6-bis(diisopropylphosphino)acenaphthene, which has similar σ-type and π-type lone-pair orbitals at the antimony atom.[37] The LUMO, HOMO, and HOMO–1 of **5** become the LUMO+1, LUMO, and HOMO of $(6)^{2+}$, respectively. This agrees well with the removal of two electrons from the HOMO of **5** in yielding $(6)^{2+}$. Expectedly, the LUMO and HOMO of **6** are the π-type orbitals located mainly at the antimony atoms of the C_4Sb_2 ring (Figure 3b). The HOMO–14 and HOMO–15 of $(6)^{2+}$ are the σ-type lone-pair orbitals at the antimony atoms.

DFT calculations at the PBEh-3c level predict singlet ground states for **5** and $(6)^{2+}$ with the singlet-triplet energy gap (ΔE_{S-T}) of 19.6 and 9.7 kcal mol^{-1}, respectively (see the Supporting Information for details). Of note, the broken-symmetry open-shell singlet (**OS**) solution for $(6)^{2+}$ was found to be 2.13 kcal mol^{-1} more stable than the closed-shell singlet (**CS**) solution. The diradical character (y), calculated according to Yamaguchi[38] by the unrestricted Hartree-Fock (UHF) method, for $(6)^{2+}$ amounts to 39%. In order to obtain more insights into the electronic structures of **5** and

Table 2: NBO charges (Q) and WBIs (PBE0/def2-TZVPP) for selected atoms and bonds of C_4Sb_2 ring, respectively, of **4**, **5**, and $(6)^{2+}$.

	4	**5**	$(6)^{2+}$
Sb_Q	1.28	0.30	0.97
C_Q	−0.18	−0.19	−0.26
Sb–C$_{WBI}$	0.73	0.89	0.99
C–C$_{WBI}$	1.56	1.44	1.42

(a)

LUMO (–1.45 eV) HOMO (–3.55 eV)

HOMO–1 (–4.68 eV) HOMO–2 (–6.42 eV)

HOMO–3 (–6.75 eV) HOMO–12 (–9.37 eV)

(b)

LUMO+1 (–2.48 eV) LUMO (–4.31 eV)

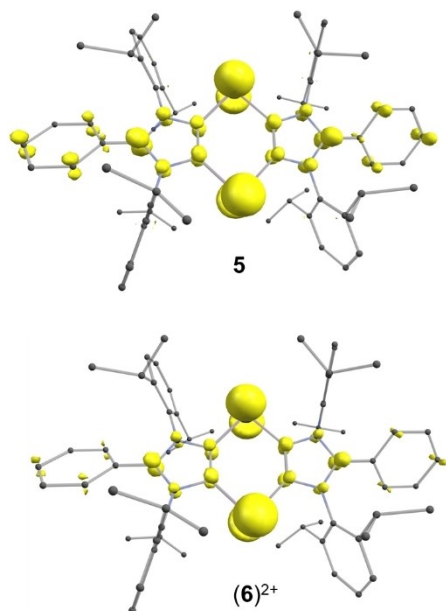HOMO (–6.53 eV) HOMO–13 (–9.31 eV)

HOMO–14 (–9.37 eV) HOMO–15 (–9.47 eV)

Figure 3. Selected frontier molecular orbitals (isosurfaces 0.05) of **5** (a) and $(6)^{2+}$ (b) calculated at RKS-PBE0/def2-TZVPP.
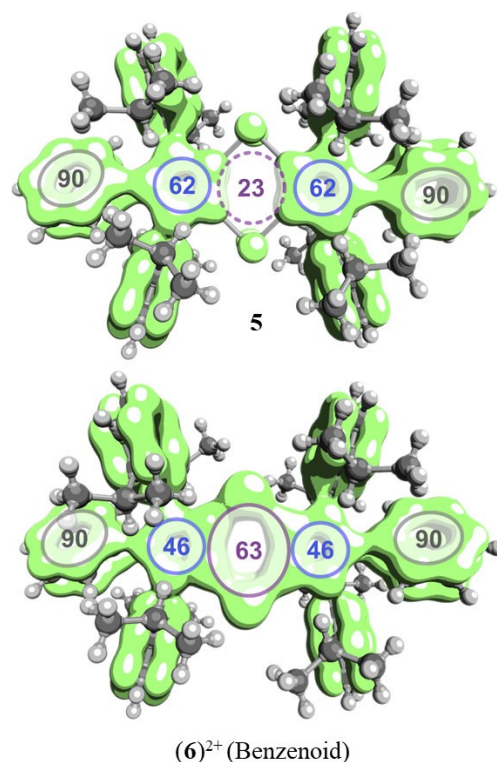
$(6)^{2+}$, we performed state-specific complete active space self-consistent field (SS-CASSCF) calculations combined with the def2-TZVPP basis set. The ground state S_0 with an active space of (6,5) for **5** has the occupation pattern 22200 (95%) and 21111 (3%) (see Supporting Information for other minor occupation patterns). For $(6)^{2+}$, the S_0 state with an active space of (4,5) has the occupation pattern 22000 (82%) and 20200 (18%). According to SS-CASSCF calculations, the diradical character (β)[39] of **5** and $(6)^{2+}$ amounts to 6% and 36%, respectively. It is worth noting that related phosphorus[10h] and arsenic[19] dications exhibit a rather small (<7%) diradical character. Thus, compound $(6)^{2+}$ may be regarded as a singlet diradicaloid that is stabilized by the delocalization of the unpaired electrons over the C_4Sb_2 ring. This would result in the formation of a 6π-electron C_4Sb_2-aromatic system in $(6)^{2+}$ (see below). Yet, it should be noted that aromaticity and diradical character are not mutually exclusive.[40]

We also performed fractional occupation number weighted density (FOD) calculations (see the Supporting Information) originally introduced by Grimme et al. as a static electron correlation (SEC) diagnostic[41] to analyze the electronic structures of **5** and **6**. FOD analyses provide reliable information on the localization of "hot" (strongly correlated and chemically active) electrons in a molecule. The FOD plots of **5** and $(6)^{2+}$ (Figure 4) nicely visualize the "hot" electrons at the antimony atoms. The resulting FOD numbers (N_{FOD}) amount to 3.07 and 2.67 e for **5** and $(6)^{2+}$, respectively. Grimme and co-workers also correlated N_{FOD} with the diradical character (y) of some singlet diradical-(oid)s.[41a] Organic compounds with a high N_{FOD} usually show a large diradical character, a direct correlation between N_{FOD} and the diradical character for main-group diradicaloids is however not obvious (see Table S11).

Various criteria have been used to assess the aromatic character of molecular rings, including the electronic-structure, magnetic response, structural and thermochemical properties.[42] In this study, we employed the electron density of delocalized bonds (EDDB) method[43] as this has been shown to be particularly well-suited for evaluating the aromaticity of molecular rings containing conjugated orbitals of atoms with a large size-dissimilarity.[44] The global (G) electron delocalization in **5** and $(6)^{2+}$ was visualized by the $EDDB_G$, which is a function of the one-electron density that represents the electrons delocalized through the system of all conjugated bonds in a molecule. To quantify the magnitude of local (P) aromaticity in individual rings of the tricyclic core of **5** and $(6)^{2+}$, we used the corresponding $EDDB_P$ function.[43a] The numbers in circles (Figure 5) refer to the percentages of the benzene aromaticity calculated using the local aromaticity index $EDDB_P$ (see Supporting Information for details). For **5**, both 1,3-imidazole rings preserve a high degree of their local aromatic character, which amounts to 62% relative to that of benzene (cf. the relative aromaticity in an isolated 1,3-imidazole ring of 63%; see the Supporting Information for other cyclic reference systems). The cyclic delocalization in the central C_4Sb_2 ring of **5** (23%) is rather small and does not support its local (anti)aromaticity. The same applies to the central C_4Sb_2 ring (13%) of the **OS** diradical form of $(6)^{2+}$ (see Figure S50), in

Figure 4. FOD plots (isosurface 0.005) of **5** and $(6)^{2+}$. Hydrogen atoms are omitted for clarity.

$(6)^{2+}$ (Benzenoid)

Figure 5. Isosurface contours ($\tau_{EDD} = 0.020$) of the global electron density of delocalized bonds ($EDDB_G$) for **5** and $(6)^{2+}$. The numbers in circles refer to the percentages of the benzene aromaticity calculated using the local aromaticity index $EDDB_P$ (see Supporting Information for details).

which local aromaticity in the 1,3-imidazole rings (54%) is also slightly reduced compared to that of **5**.

In turn, the central C_4Sb_2 ring (63%) of the **CS** benzenoid form of $(6)^{2+}$ (Figure 5) is essentially aromatic, which comes at the cost of further reduction of the local aromaticity in the 1,3-imidazole rings (46%). It should be noted that aromaticity and diradical character are not mutually exclusive[40] and almost all cyclic main-group diradicaloids featuring Hückel's $[4n+2]$ π-electron systems are mostly aromatic.[36b,c,45] Thus, the EDDB method predicts the resonance electronic structures of **5** (as well as the pure **OS** diradical form of $(6)^{2+}$) to be well represented by the Clar structures with two π-sextets fixed in the imidazole rings. In contrast, the **CS** benzenoid form of $(6)^{2+}$ is globally aromatic and suggests the resonance electronic structure with a migrating π-sextet. $(6)^{2+}$ may formally be regarded as an iso(valence)electronic (14 π-electrons) to anthracene. For anthracene, a similar description of migrating π-sextets is commonly accepted. In anthracene, the effectiveness of cyclic delocalization of electrons according to EDDB amounts to 39% for the terminal rings and 59% for the central one.[46]

We also investigated aromaticity of **5**, $(6)^{2+}$, and selected reference cyclic compounds by the conventional methods namely $MCI^{2/N}$ (normalized multicenter index), PDI (para-delocalization index), NICS (nucleus independent chemical shift), and ACID (anisotropy of the induced current density) (see the Supporting Information for details). The local aromaticity predictions by these descriptions are in line with the findings by the EDDB method (see Tables S12 and S13).

Having analyzed the electronic structures of **5** and **6**, we prompted to explore their reactivity. Treatments of **6** with PhEEPh (E = S, Se) yielded $[(ADC)SbEPh]_2[B(C_6F_5)_4]_2$ (7-E) as yellow crystalline solids (**7-S** 93%, **7-Se** 94%) (Scheme 2a). The ^1H and ^{13}C NMR spectra of **7-E** show expected signals for the ADC moiety. The solid-state molecular structure of **7-S** features SPh substituents in *E*-configuration. The exact mechanism of the formation of *E*-isomers of **7-E** is currently not known. As suggested for known main-group diradicaloids,[36] step-wise reactions involving either radicals (PhE•) or ions (PhE+ and PhE−), generated via homolytic or heterolytic E–E bond cleavage, with **6** are likely. The C–Sb bond lengths of **7-S** (av.

2.166(2) Å) are larger than those of **6** but are akin to those of **5** (Table 1).

Reaction of **5** and (cod)Mo(CO)$_4$ at room temperature afforded $[\{(ADC)Sb\}_2\{Mo(CO)_4\}]$ (**8**) as a brown crystalline solid in 99% yield (Scheme 2b). The molecular structure of **8** (Scheme 2b) shows a distorted octahedral geometry at the molybdenum atom. The fold angle along the antimony atoms of the C_4Sb_2 ring is 115.9(1)°. They bind to the Mo atom in *cis*-fashion. In addition to the anticipated ^1H and $^{13}C\{^1H\}$ NMR signals for the ADC moieties, the ^{13}C NMR spectrum of **8** exhibits one resonance at 201.7 ppm for the CO ligands. The IR spectrum of **8** (Figure S29) shows four CO stretching bands as expected for a *cis*-(L)$_2$M(CO)$_4$ complex, which may be assigned as A_2^1 (medium, 1966 cm^{-1}), B_1 (shoulder, 1925 cm^{-1}), A_1^1 (strong, 1850 cm^{-1}), and B_2 (strong, 1813 cm^{-1}).[47] Each of the antimony atoms of **8** has trigonal pyramidal geometry with the sum of the angles of ca. 270.1°, consistent with the presence of a lone-pair.

Conclusion

In conclusion, the first 1,4-distibabenzene-1,4-diide (**5**), which may also be regarded as a base-stabilized cyclic bis-stibinidene, has been reported as a crystalline solid. Two electron oxidation of **5** affords the 1,3-imidazole-fused 1,4-distibabenzene derivative **6** with a formally 6π-electron central C_4Sb_2 ring. The calculated diradical character of $(6)^{2+}$ amounts to 39% (according to UHF) or 36% (according to SS-CASSCF). The broken-symmetry **OS** solution for $(6)^{2+}$ is found to be 2.13 kcal mol^{-1} more stable than the **CS** solution. As suggested by EDDB and others descriptors, noticeable diradical character of $(6)^{2+}$ is due to the local aromatic stabilization in imidazole rings that comes at the cost of local aromaticity in the C_4Sb_2 ring, which in turn predominates in the **CS** configuration. The paucity of heavier main-group analogues of benzene and related annulated heterocycles may be rationalized considering their potential open-shell electronic structures originated primarily from rather weak C–E π-interactions. Compound **6** represents the first example of a stable 1,4-distibabenzene (as well as stibabenzene in general) derivative known to
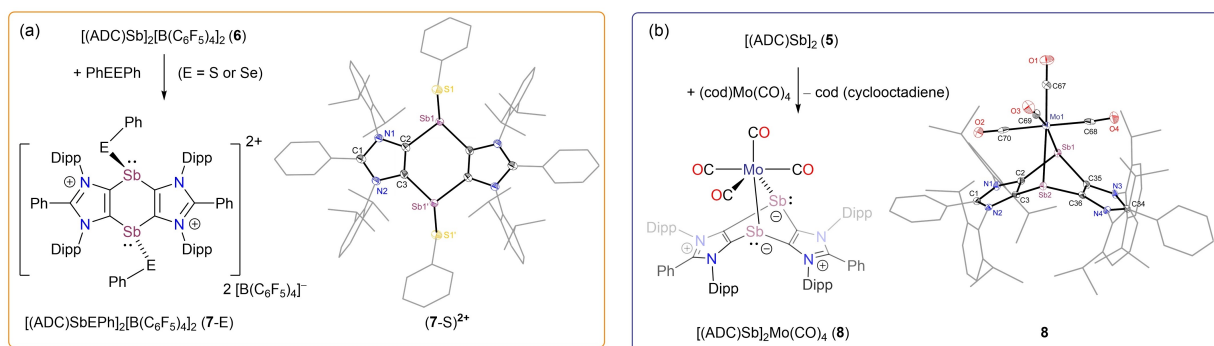
Scheme 2. Synthesis and solid-state molecular structures (measured at 100 K) of **7-E** (a) and **8** (b). Only the dicationic part is shown for **7-S**. Aryls are shown as wire-frames. H atoms and solvent molecules have been omitted for clarity. Thermal ellipsoids are shown at 50% probability.

date. Preliminary reactivity of **5** and **6** has been shown with PhEEPh and (cod)Mo(CO)$_4$ to access **7**-E and **8**, respectively. These results show the versatility of ADC in accessing innovative molecular structures, which have been hitherto considered as challenging synthetic targets.

Acknowledgements

Conflict of Interest

The authors declare no conflict of interest.

Data Availability Statement

The data that support the findings of this study are available in the Supporting Information of this article.

Keywords: Antimony · Aromaticity · Carbene · Diradicaloid · Heterocycle

[1] a) H. Borns, *Nature* **1925**, *116*, 48–48; b) E. H. Tripp, *Nature* **1925**, *115*, 909–909; c) L. C. Newell, *J. Chem. Educ.* **1926**, *3*, 1248; d) E. Hückel, *Grundzüge der Theorie ungesättigter und aromatischer Verbindungen*, Verlag Chemie, Berlin, **1938**.

[2] a) N. Tokitoh, *Acc. Chem. Res.* **2004**, *37*, 86–94; b) I. Fernández, G. Frenking, G. Merino, *Chem. Soc. Rev.* **2015**, *44*, 6452–6463; c) C. W. Landorf, M. M. Haley, *Angew. Chem. Int. Ed.* **2006**, *45*, 3914–3936; *Angew. Chem.* **2006**, *118*, 4018–4040; d) D. Chen, Y. Hua, H. Xia, *Chem. Rev.* **2020**, *120*, 12994–13086; e) K. Ota, R. Kinjo, *Chem. Soc. Rev.* **2021**, *50*, 10594–10673; f) G. He, O. Shynkaruk, M. W. Lui, E. Rivard, *Chem. Rev.* **2014**, *114*, 7815–7880.

[3] a) A. J. Ashe in *Comprehensive Heterocyclic Chemistry III* (Eds.: A. R. Katritzky, C. A. Ramsden, E. F. V. Scriven, R. J. K. Taylor), Elsevier, Oxford, **2008**, pp. 1039–1048; b) A. J. Ashe III, *Eur. J. Inorg. Chem.* **2016**, 572–574; c) A. J. Ashe III, *Top. Curr. Chem.* **1982**, *105*, 125–155; d) A. J. Ashe, *Acc. Chem. Res.* **1978**, *11*, 153–157; e) L. Weber, F. Ebeler, R. S. Ghadwal, *Coord. Chem. Rev.* **2022**, *461*, 214499; f) P. P. Power, *Organometallics* **2020**, *39*, 4127–4138; g) J. D. Protasiewicz in *Comprehensive Inorganic Chemistry II: From Elements to Applications, Vol. 1*, 2nd ed. (Ed.: K. Poeppelmeier), Elsevier, Amsterdam, **2013**, pp. 325–348; h) C. Jones, *Coord. Chem. Rev.* **2001**, *215*, 151–169.

[4] a) I. Păuşescu, M. Medeleanu, M. Ştefănescu, F. Peter, R. Pop, *Heteroat. Chem.* **2015**, *26*, 206–214; b) R. Salcedo, *J. Mol. Struct.: TheoChem* **2004**, *674*, 125–129.

[5] J. E. Walley, L. S. Warring, G. Wang, D. A. Dickie, S. Pan, G. Frenking, R. J. Gilliard, Jr., *Angew. Chem. Int. Ed.* **2021**, *60*, 6682–6690; *Angew. Chem.* **2021**, *133*, 6756–6764.

[6] P. C. Andrews, J. E. McGrady, P. J. Nichols, *Organometallics* **2004**, *23*, 446–453.

[7] a) L. Weber, *Eur. J. Inorg. Chem.* **2007**, 4095–4117; b) H. Ramdane, H. Ranaivonjatovo, J. Escudié, N. Knouzi, *Organometallics* **1996**, *15*, 2683–2684; c) M. Driess, H. Pritzkow, M. Sander, *Angew. Chem. Int. Ed. Engl.* **1993**, *32*, 283–285; *Angew. Chem.* **1993**, *105*, 273–275.

[8] a) R. Pietschnig, A. Orthaber, *Reference Module in Chemistry, Molecular Sciences and Chemical Engineering*, Elsevier, Amsterdam, **2016**, https://doi.org/10.1016/B978-0-12-409547-2.11721-4; b) P. L. Floch, *Coord. Chem. Rev.* **2006**, *250*, 627–681; c) L. Weber, *Coord. Chem. Rev.* **2005**, *249*, 741–763; d) L. Weber, *Eur. J. Inorg. Chem.* **2000**, 2425–2441.

[9] G. Märkl, *Angew. Chem. Int. Ed. Engl.* **1966**, *5*, 846–847; *Angew. Chem.* **1966**, *78*, 906–906.

[10] a) R. L. Falconer, C. A. Russell, *Coord. Chem. Rev.* **2015**, *297–298*, 146–167; b) N. S. Townsend, S. R. Shadbolt, M. Green, C. A. Russell, *Angew. Chem. Int. Ed.* **2013**, *52*, 3481–3484; *Angew. Chem.* **2013**, *125*, 3565–3568; c) N. A. Piro, C. C. Cummins, *Angew. Chem. Int. Ed.* **2009**, *48*, 934–938; *Angew. Chem.* **2009**, *121*, 952–956; d) Y. Canac, D. Bourissou, A. Baceiredo, H. Gornitzka, W. W. Schoeller, G. Bertrand, *Science* **1998**, *279*, 2080–2082; e) O. J. Scherer, H. Sitzmann, G. Wolmershäuser, *Angew. Chem. Int. Ed. Engl.* **1985**, *24*, 351–353; *Angew. Chem.* **1985**, *97*, 358–359; f) A. J. Ashe, *J. Am. Chem. Soc.* **1971**, *93*, 3293–3295; g) C. Müller, L. E. E. Broeckx, I. de Krom, J. J. M. Weemers, *Eur. J. Inorg. Chem.* **2013**, 187–202; h) D. Rottschäfer, B. Neumann, H.-G. Stammler, T. Sergeieva, D. M. Andrada, R. S. Ghadwal, *Chem. Eur. J.* **2021**, *27*, 3055–3064; i) A. Koner, G. Pfeifer, Z. Kelemen, G. Schnakenburg, L. Nyulászi, T. Sasamori, R. Streubel, *Angew. Chem. Int. Ed.* **2017**, *56*, 9231–9235; *Angew. Chem.* **2017**, *129*, 9359–9363.

[11] a) N. T. Coles, A. Sofie Abels, J. Leitl, R. Wolf, H. Grützmacher, C. Müller, *Coord. Chem. Rev.* **2021**, *433*, 213729; b) J. J. M. Weemers, W. N. P. van der Graaff, E. A. Pidko, M. Lutz, C. Müller, *Chem. Eur. J.* **2013**, *19*, 8991–9004.

[12] T. Ishii, K. Suzuki, T. Nakamura, M. Yamashita, *J. Am. Chem. Soc.* **2016**, *138*, 12787–12790.

[13] A. J. Ashe III, *J. Am. Chem. Soc.* **1971**, *93*, 6690–6691.

[14] A. J. Ashe III, T. R. Diephouse, M. Y. El-Sheikh, *J. Am. Chem. Soc.* **1982**, *104*, 5693–5699.

[15] F. Bickelhaupt, R. Lourens, H. Vermeer, R. J. M. Weustink, *Recl. Trav. Chim. Pays-Bas* **1979**, *98*, 3–4.

[16] a) J. Dosso, B. Bartolomei, N. Demitri, F. P. Cossío, M. Prato, *J. Am. Chem. Soc.* **2022**, *144*, 7295–7301; b) X.-Y. Wang, M. Richter, Y. He, J. Björk, A. Riss, R. Rajesh, M. Garnica, F. Hennersdorf, J. J. Weigand, A. Narita, R. Berger, X. Feng, W. Auwärter, J. V. Barth, C.-A. Palma, K. Müllen, *Nat. Commun.* **2017**, *8*, 1948; c) J. Nagasaki, S. Hiroto, H. Shinokubo, *Chem. Asian J.* **2017**, *12*, 2311–2317.

[17] a) D. Rottschäfer, F. Ebeler, T. Strothmann, B. Neumann, H.-G. Stammler, A. Mix, R. S. Ghadwal, *Chem. Eur. J.* **2018**, *24*, 3716–3720; b) N. K. T. Ho, B. Neumann, H.-G. Stammler, V. H. Menezes da Silva, D. G. Watanabe, A. A. C. Braga, R. S. Ghadwal, *Dalton Trans.* **2017**, *46*, 12027–12031; c) R. S. Ghadwal, S. O. Reichmann, R. Herbst-Irmer, *Chem. Eur. J.* **2015**, *21*, 4247–4251.

[18] D. Rottschäfer, S. Blomeyer, B. Neumann, H.-G. Stammler, R. S. Ghadwal, *Chem. Sci.* **2019**, *10*, 11078–11085.

[19] D. Rottschäfer, T. Glodde, B. Neumann, H. G. Stammler, D. M. Andrada, R. S. Ghadwal, *Angew. Chem. Int. Ed.* **2021**, *60*, 15849–15853; *Angew. Chem.* **2021**, *133*, 15983–15987.

[20] M. K. Sharma, F. Ebeler, T. Glodde, B. Neumann, H.-G. Stammler, R. S. Ghadwal, *J. Am. Chem. Soc.* **2021**, *143*, 121–125.

[21] a) M. K. Sharma, D. Rottschäfer, T. Glodde, B. Neumann, H. G. Stammler, R. S. Ghadwal, *Angew. Chem. Int. Ed.* **2021**, *60*, 6414–6418; *Angew. Chem.* **2021**, *133*, 6485–6489; b) M. K. Sharma, T. Glodde, B. Neumann, H.-G. Stammler, R. S. Ghadwal, *Chem. Eur. J.* **2020**, *26*, 11113–11118.

[22] Compound **3** was generated in situ on treatment of (IPr^Ph)Cl (**1**) with *n*BuLi and subsequent silylation of the anionic dicarbene Li(ADC^Ph) (**2**) with Me₃SiCl.

[23] a) M. S. M. Philipp, M. J. Krahfuss, K. Radacki, U. Radius, *Eur. J. Inorg. Chem.* **2021**, 4007–4019; b) A. Sidiropoulos, B. Osborne, A. N. Simonov, D. Dange, A. M. Bond, A. Stasch, C. Jones, *Dalton Trans.* **2014**, *43*, 14858–14864; c) R. Kretschmer, D. A. Ruiz, C. E. Moore, A. L. Rheingold, G. Bertrand, *Angew. Chem. Int. Ed.* **2014**, *53*, 8176–8179; *Angew. Chem.* **2014**, *126*, 8315–8318; d) C. L. Dorsey, R. M. Mushinski, T. W. Hudnall, *Chem. Eur. J.* **2014**, *20*, 8914–8917; e) F. D. Henne, A. T. Dickschat, F. Hennersdorf, K. O. Feldmann, J. J. Weigand, *Inorg. Chem.* **2015**, *54*, 6849–6861.

[24] R. Deka, A. Orthaber, *Dalton Trans.* **2022**, *51*, 8540–8556.

[25] a) M. S. M. Philipp, U. Radius, *Z. Anorg. Allg. Chem.* **2022**, *648*, e202200085; b) J. Krüger, C. Wölper, L. John, L. Song, P. R. Schreiner, S. Schulz, *Eur. J. Inorg. Chem.* **2019**, 1669–1678; c) D. Raiser, K. Eichele, H. Schubert, L. Wesemann, *Chem. Eur. J.* **2021**, *27*, 14073–14080.

[26] M. M. Siddiqui, S. K. Sarkar, M. Nazish, M. Morganti, C. Köhler, J. Cai, L. Zhao, R. Herbst-Irmer, D. Stalke, G. Frenking, H. W. Roesky, *J. Am. Chem. Soc.* **2021**, *143*, 1301–1306.

[27] P. Šimon, F. de Proft, R. Jambor, A. Růžička, L. Dostál, *Angew. Chem. Int. Ed.* **2010**, *49*, 5468–5471; *Angew. Chem.* **2010**, *122*, 5600–5603.

[28] a) L. Dostál, *Coord. Chem. Rev.* **2017**, *353*, 142–158; b) I. Vránová, V. Kremlacek, M. Erben, J. Turek, R. Jambor, A. Ruzicka, M. Alonso, L. Dostal, *Dalton Trans.* **2017**, *46*, 3556–3568; c) I. Vránová, M. Alonso, R. Jambor, A. Růžička, M. Erben, L. Dostál, *Chem. Eur. J.* **2016**, *22*, 7376–7380.

[29] The related triflate derivative prepared using **5** and AgOTf was found to be rather unstable and could not be satisfactorily characterized.

[30] Deposition Numbers 2206010 (for **4**), 2206011 (for **5**), 2206012 (for **6**), 2206013 (for **7**-S) and 2206014 (for **8**) contains the supplementary crystallographic data for this paper. These data are provided free of charge by the joint Cambridge Crystallographic Data Centre and Fachinformationszentrum Karlsruhe Access Structures service.

[31] P. Pyykkö, M. Atsumi, *Chem. Eur. J.* **2009**, *15*, 186–197.

[32] S. S. Batsanov, *Inorg. Mater.* **2001**, *37*, 871–885.

[33] A. Merschel, D. Rottschäfer, B. Neumann, H.-G. Stammler, R. S. Ghadwal, *Organometallics* **2020**, *39*, 1719–1729.

[34] C. Elschenbroich, *Teubner Studienbücher Chemie: Organometallchemie, Vol. 6., überarbeitete Auflage*, Vieweg+Teubner Verlag, Wiesbaden, **2008**.

[35] K. D. Dobbs, J. E. Boggs, A. H. Cowley, *Chem. Phys. Lett.* **1987**, *141*, 372–375.

[36] a) H. Steffenfauseweh, Y. V. Vishnevskiy, B. Neumann, H. G. Stammler, D. M. Andrada, R. S. Ghadwal, *Angew. Chem. Int. Ed.* **2022**, *61*, e202207415; *Angew. Chem.* **2022**, *134*, e202207415; b) J. Bresien, L. Eickhoff, A. Schulz, E. Zander in *Reference Module in Chemistry, Molecular Sciences and Chemical Engineering*, Elsevier, Amsterdam, **2021**, https://doi.org/10.1016/B978-0-12-823144-9.00029-7; c) T. Stuyver, B. Chen, T. Zeng, P. Geerlings, F. De Proft, R. Hoffmann, *Chem. Rev.* **2019**, *119*, 11291–11351.

[37] V. Kumar, R. G. Gonnade, C. B. Yildiz, M. Majumdar, *Angew. Chem. Int. Ed.* **2021**, *60*, 25522–25529; *Angew. Chem.* **2021**, *133*, 25726–25733.

[38] a) M. Nakano, R. Kishi, N. Nakagawa, S. Ohta, H. Takahashi, S.-i. Furukawa, K. Kamada, K. Ohta, B. Champagne, E. Botek, S. Yamada, K. Yamaguchi, *J. Phys. Chem. A* **2006**, *110*, 4238–4243; b) K. Yamaguchi, M. Okumura, K. Takada, S. Yamanaka, *Int. J. Quantum Chem.* **1993**, *48*, 501–515.

[39] a) W. D. Laidig, H. F. Schaefer III, *J. Chem. Phys.* **1981**, *74*, 3411–3414; b) E. Miliordos, K. Ruedenberg, S. S. Xantheas, *Angew. Chem. Int. Ed.* **2013**, *52*, 5736–5739; *Angew. Chem.* **2013**, *125*, 5848–5851.

[40] B. Braïda, A. Lo, P. C. Hiberty, *ChemPhysChem* **2012**, *13*, 811–819.

[41] a) C. A. Bauer, A. Hansen, S. Grimme, *Chem. Eur. J.* **2017**, *23*, 6150–6164; b) S. Grimme, A. Hansen, *Angew. Chem. Int. Ed.* **2015**, *54*, 12308–12313; *Angew. Chem.* **2015**, *127*, 12483–12488.

[42] I. Fernandez, *Aromaticity: Modern Computational Methods and Applications*, Elsevier, Amsterdam, **2021**, https://doi.org/10.1016/C2019-0-04193-3.

[43] a) D. W. Szczepanik, M. Andrzejak, J. Dominikowska, B. Pawełek, T. M. Krygowski, H. Szatylowicz, M. Solà, *Phys. Chem. Chem. Phys.* **2017**, *19*, 28970–28981; b) D. W. Szczepanik, M. Andrzejak, K. Dyduch, E. Żak, M. Makowski, G. Mazur, J. Mrozek, *Phys. Chem. Chem. Phys.* **2014**, *16*, 20514–20523.

[44] D. W. Szczepanik, M. Solà, *ChemistryOpen* **2019**, *8*, 219–227.

[45] a) S. González-Gallardo, F. Breher in *Comprehensive Inorganic Chemistry II*, 2nd ed. (Eds.: J. Reedijk, K. Poeppelmeier), Elsevier, Amsterdam, **2013**, pp. 413–455; b) F. Breher, *Coord. Chem. Rev.* **2007**, *251*, 1007–1043; c) H. Grützmacher, F. Breher, *Angew. Chem. Int. Ed.* **2002**, *41*, 4006–4011; *Angew. Chem.* **2002**, *114*, 4178–4184; d) M. Abe, *Chem. Rev.* **2013**, *113*, 7011–7088; e) M. Abe, J. Ye, M. Mishima, *Chem. Soc. Rev.* **2012**, *41*, 3808–3820; f) K. Chandra Mondal, S. Roy, H. W. Roesky, *Chem. Soc. Rev.* **2016**, *45*, 1080–1111; g) Z. Zeng, X. Shi, C. Chi, J. T. Lopez Navarrete, J. Casado, J. Wu, *Chem. Soc. Rev.* **2015**, *44*, 6578–6596.

[46] D. W. Szczepanik, M. Solà, T. M. Krygowski, H. Szatylowicz, M. Andrzejak, B. Pawełek, J. Dominikowska, M. Kukułka, K. Dyduch, *Phys. Chem. Chem. Phys.* **2018**, *20*, 13430–13436.

[47] J. A. Vlček, F. Baumann, W. Kaim, F.-W. Grevels, F. Hartl, *J. Chem. Soc. Dalton Trans.* **1998**, 215–220.